

1 *Supporting Information for*

2 **Application of a new UAV measurement methodology to**
3 **the quantification of CO₂ and CH₄ emissions from a**
4 **major coking plant**

5
6 Tianran Han¹, Conghui Xie¹, Yayong Liu¹, Yanrong Yang¹, Yuheng Zhang¹, Yufei
7 Huang¹, Xiangyu Gao², Xiaohua Zhang³, Fangmin Bao⁴, Shao-Meng Li¹

8
9 ¹ State Key Joint Laboratory of Environmental Simulation and Pollution Control, College of
10 Environmental Sciences and Engineering, Peking University, Beijing 100871, P.R. China

11 ² Beijing Wisdominc Technology Co., Ltd., Beijing, P.R. China

12 ³ Suzhou Environmental Monitoring Center, Jiangsu Province, P.R. China

13 ⁴ Jiangsu Shagang Group Co., Ltd., Beijing, P.R. China

14 *Correspondence to:* Shao-Meng Li (shaomeng.li@pku.edu.cn)

15 **Section SI-1. TERRA-based determination of CH₄ and CO₂ emission rates**

16 CH₄ and CO₂ emission rates for the surveyed coking plant were determined using the Top-down
17 Emission Rate Retrieval Algorithm (TERRA)(Gordon et al., 2015), which computes integrated mass
18 fluxes through airborne virtual box/screen measurements including those made from aircraft and in this
19 case UAVs. To run TERRA based on a virtual box flight, the first step is to map the CH₄ and CO₂ mixing
20 ratio data measured along the level flight tracks encircling a facility to the two-dimensional virtual walls
21 of the virtual box, created from stacking the level flight tracks, that surrounds the facility. The two-
22 dimensional virtual walls (or screens) are derived from the unwrapping of the virtual box, to assist the
23 presentation of the CH₄ and CO₂ plumes along the flight tracks, with the horizontal path length (i.e., the
24 ground line projection of the fitted flight track) and altitude as the two dimensions. The start of the
25 horizontal path is typically defined as the south-east corner of the virtual box, but the selection of this
26 starting position has no effect on the emission rate computation, and the horizontal path distance
27 increases in a counter clockwise direction. Subsequently, TERRA applies the Simple Kriging algorithm
28 to interpolate the data and produces a mesh on the virtual box walls whose resolution can be set depending
29 on applications, e.g., at 20 m (vertical) by 40 m (horizontal) for aircraft measurements. For the modified
30 version of TERRA applied to the UAV measurements in this study, the mesh has been adjusted to a size
31 of 1 m (vertical) by 2 m (horizontal), as UAVs fly significantly shorter distances compared to piloted

32 aircraft. The mixing ratios of both CH₄ and CO₂ are extrapolated from the lowest flight altitudes to the
 33 ground digital elevation using one of several methods or a combination thereof, namely (1) assuming a
 34 constant (2) linear extrapolation between a constant and background (3) a background value below flight
 35 altitudes (4) linear fit between the lowest flight altitude and zero at the ground and (5) exponential fit
 36 from the lower flight altitudes(Gordon et al., 2015). In this study, CH₄ was extrapolated to the ground
 37 mostly using linear and exponential fits that best describe the vertical mixing of ground-based plumes
 38 such as emission of CH₄. Concurrently measured wind speed from the UAV(Yang, 2023) is decomposed
 39 into two components (parallel and normal to the flight tracks) based on the wind direction and similarly
 40 interpolated onto the 1 m x 2 m mesh. The decomposed wind speeds are further extrapolated to the
 41 ground digital elevation using a log profile fit(Gordon et al., 2015). Based on the
 42 interpolated/extrapolated CH₄ and CO₂ mixing ratio, temperature, pressure, and wind speeds, TERRA
 43 computes the fluxes of CH₄ and CO₂ through the virtual walls and finally their facility emission rates by
 44 integrating the fluxes.

45 To summarize, in TERRA the mass-balance in computing the emissions within a control box for a
 46 given inert pollutant such as CH₄ or CO₂ is presented by:

$$47 \quad E_C = E_{C,H} + E_{C,V} - E_{C,M} \quad (1)$$

48 where E_C is the emission rate, $E_{C,H}$ is the horizontal advective transfer rate through the box walls, $E_{C,V}$
 49 is the advective transfer rate through the box top and $E_{C,M}$ is the increase in mass within the volume due
 50 to a change in air density. The vertical transfer rate term $E_{C,V}$ is estimated by computing the air mass
 51 vertical transfer rate, determined from vertical wind estimated from air mass balance within the box, and
 52 multiplying it with the CO₂ or CH₄ mixing ratios at the box top. This term is normally negligible in top-
 53 down emission estimate approaches since it is typically miniscule compared to horizontal fluxes, but can
 54 affect the computed emission rates when vertical air movement becomes more significant such as under
 55 unstable atmospheric conditions. $E_{C,M}$ is often ignored in other mass-balance approaches; in TERRA it
 56 is estimated by taking the time derivative of the ideal gas law in temperature and pressure during the
 57 flight time, and typically it does not change significantly over the duration of 30 minutes or so for the
 58 UAV flight.

59 TERRA has been updated at Peking University now with an embedded routine to automatically fit
60 flight tracks, a critical first step in the computation and a procedure previously conducted offline through
61 geographic information system (GIS) when using TERRA. The updated algorithm is now recoded using
62 the Python language and runs under a browser-server environment with a new GUI and new interactive
63 data flow. This updated algorithm is named the Mass Emission and Transfer Rate Evaluation System
64 (METRES) and is copyrighted.

65 **Section SI-2. Uncertainty estimation**

66 To determine the overall uncertainty in the emission rates, each source of uncertainty contributing
67 to the overall uncertainty needs to be identified and quantified. For the emission rate quantification from
68 UAV measurement, the sources of uncertainties include: measurement uncertainties in the mixing ratios
69 and wind speeds (δ_M), the near-surface wind extrapolation (δ_{Wind}), the near-surface mixing ratio
70 extrapolation (δ_{Ex}), box-top mixing ratio (δ_{Top}), box-top height (δ_{BH}) and uncertainties due to data
71 deconvolution as shown in the main text (δ_{Deconv}). Each uncertainty is treated as an independent estimate,
72 and all uncertainties are propagated in quadrature to determine the overall uncertainty in the estimated
73 emission rate:

$$74 \quad \delta^2 = \delta_M^2 + \delta_{Wind}^2 + \delta_{Ex}^2 + \delta_{Top}^2 + \delta_{BH}^2 + \delta_{Deconv}^2 \quad (2)$$

75 CH₄ and CO₂ measurement uncertainties from the instrument are <1%. In a previous study(Gordon
76 et al., 2015), a Monte Carlo simulation was used to demonstrate that the uncertainties due to wind speed
77 and mixing ratio measurement uncertainty are both approximately 1%. The uncertainty for wind speed
78 extrapolation is also conservatively estimated as $\delta_{Wind} \approx 1\%$ for all cases. Due to a lack of near-surface
79 measurements along the box walls, extrapolation of CH₄ and mixing ratios from the lowest flight path (~
80 150 m above ground level) to the ground level has been shown to be a source of potentially large
81 uncertainty within TERRA. The magnitude of the uncertainty depends on the nature of the emissions;
82 for example, surface emissions which may not be fully captured by the flight range have higher
83 uncertainties $\approx 20\%$, whereas elevated stack emissions which are fully captured by the flight range lead
84 to negligible uncertainties of <4% in the emission estimates(Gordon et al., 2015). To estimate
85 uncertainties due to mixing ratio extrapolation, results from other extrapolation techniques (i.e., linear to

86 the ground, constant value to the ground, linear to background value, or some combination of methods)
 87 were derived and compared with the result from background below flight extrapolation.

88 Additional components contributing to uncertainties specific to box approach include box-top
 89 mixing ratio (δ_{Top}) and box-top height (δ_{BH}). The TERRA box approach assumes a constant mixing ratio
 90 at the box top by averaging the measured value at the top level. The term δ_{Top} is determined from the
 91 95% confidence interval ($2\sigma/\sqrt{n}$) of the interpolated measurements. The uncertainty due to the choice of
 92 box height, δ_{BH} , within TERRA is estimated by recalculating the emission rate with a reduced box height
 93 of 100 m. For cases that use the air sampling system instead of online measuring instruments, as the CH₄
 94 and CO₂ time series measured from the air sampler were deconvoluted to restore the unsmoothed time
 95 series before being input into the TREEA algorithm, it is necessary to account for the uncertainty that
 96 comes from such deconvolution as outlined in the main text. Time series before and after deconvolution
 97 were applied to the TERRA algorithm to obtain the total emission rates, calculation shows that emission
 98 rates before and after deconvolution vary within 1%. To this end, the uncertainty for time series
 99 deconvolution is conservatively estimated as $\delta_{Wind} \approx 1\%$. The assessment of uncertainties for the
 100 TERRA-computed emission rates from the coking plant are listed in Table S1.

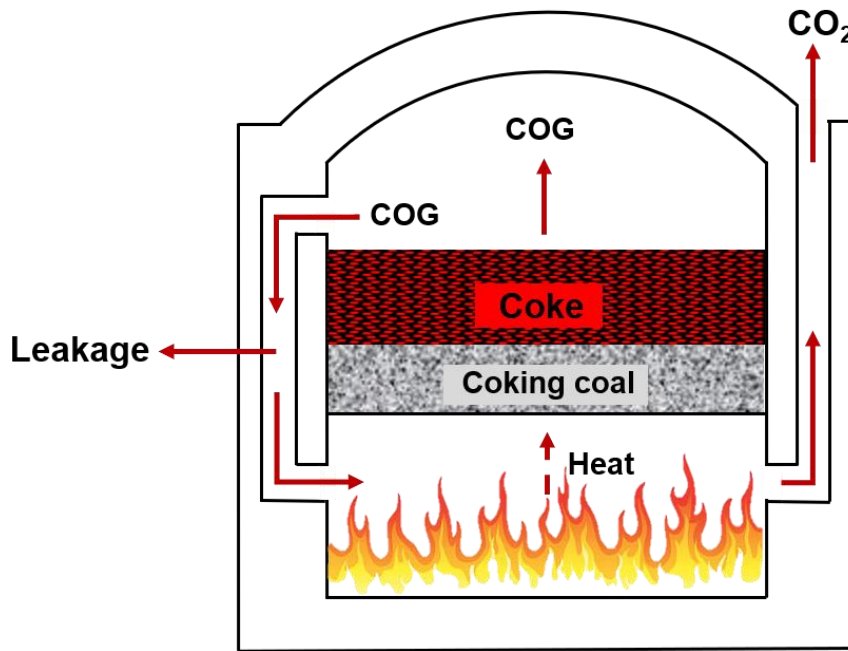
101 **Table S1.** Assessment of percent uncertainties for CH₄ and CO₂ emission estimations from the two coking plant
 102 stacks

	CH ₄ (%)	CO ₂ (%)
δ_M	1	1
δ_{Wind}	1	1
δ_{Ex}	2	6
δ_{Top}	8	3
δ_{BH}	8	16
δ_{Deconv}	1	1
δ	12	17

109

110 **Section SI-3. Evaluation of CO₂ emissions through carbon material balance**

111 Figure S1 illustrates the coking process flow and the structure of a coking oven. Coking is a process
112 in which coking coal is heated in an oxygen-free environment to produce coke, a high-carbon
113 metallurgical coke used in steel production. The process takes place in a coke oven, where coking coal
114 is heated at temperatures exceeding 1000 degrees Celsius, driving off all volatile components of the coal
115 and leaving behind coke. Coke oven gas (COG), the byproduct of coking, is mainly composed of the
116 components listed in Table S2(Razzaq et al., 2013). This gas is recovered and mostly reused as the fuel
117 in firing the coke oven to maintain the high temperatures needed for coking(Zhang, 2019),
118 reducing/eliminating the need for external fuel sources. However, burning COG generates CO₂, which is
119 the primary waste gas emitted.



120

121

Figure S1. The conceptual coking process flow and the structure of the coking oven

122

Table S2. Main carbon constitutes and their corresponding compositions (vol%) in coke oven gas

Component	Content
CH ₄	23~27%
CO ₂	1.5~3%
CO	5~8%
C ₂ H ₄	2~4%

123 The main products of coking are coke, COG, and slag. In Chinese coking plants(Zhang, 2019),
 124 typically half of the produced COG is used as fuel in firing the coke oven, while a small portion is
 125 recycled for producing chemical products, and the rest is either leaked (5%)(Hein, 2012) or an unknown
 126 fraction is directly released into the atmosphere. The Shagang coking plant has implemented a process
 127 for recycling slag. This process involves reusing the slag, which is generated during the coking process,
 128 as part of the fuel for the coking oven. As a result, the carbon in the slag is similarly oxidized into CO₂
 129 and subsequently released into the atmosphere as well. Therefore, the CO₂ emissions (E_{CO_2}) mainly come
 130 from the combustion of COG ($E_{\text{combustion-COG}}$), the combustion of slag ($E_{\text{combustion-slag}}$), and the direct
 131 release of COG (E_{release}):

$$132 \quad E_{CO_2} = E_{\text{combustion-COG}} + E_{\text{combustion-slag}} + E_{\text{release}} \quad (3)$$

133 Based on the carbon material balance, the amount of carbon in COG combusted in the coking oven
 134 ($C_{\text{combustion-COG}}$) during the coking process can be derived from material balance:

$$135 \quad C_{\text{combustion-COG}} = \alpha(C_{\text{coal}} - C_{\text{coke}} - C_{\text{slag}}) \quad (4)$$

136 where C_{coal} is the amount of carbon in coal, C_{coke} the amount in coke, and C_{slag} the amount in slag.
 137 α is the fraction of COG used in firing the coking oven and is 0.5 based on operation data at the Shagang
 138 coking plant. The measured coking plant consists of two coke oven batteries, each with its own stack.
 139 Each coking oven battery produced 127.8 t coke hr⁻¹, thus totalling 255.6 t coke hr⁻¹ (p_{coke}) between the
 140 two batteries during the UAV measurement period with a coke yield of 78.5%. The carbon content of
 141 coking coal typically ranges from 80% to 87%(Dai et al., 2022). Assuming an average value of 83.5%,
 142 the total amount of carbon in the coking coal used by the coking plant per hour can be calculated as:

$$143 \quad C_{\text{coal}} = \frac{p_{\text{coke}}}{78.5\%} \times 83.5\% = 272 \text{ t C hr}^{-1} \quad (5)$$

144 according to the US EPA, metallurgical coke has a carbon content of 82 to 87%(U.S. Environmental
 145 Protection Agency, 2008). If an average value of 84.5% is taken, the produced carbon in the coke during
 146 the coking process can be calculated as:

$$147 \quad C_{\text{coke}} = p_{\text{coke}} \times 84.5\% = 216 \text{ t C hr}^{-1} \quad (6)$$

148 Generally speaking, the yield of slag is 0.05% to 0.07% of the coal charged for coking process (an
 149 average value of 0.06% is taken here), and that the carbon content of slag is around 80%(Li, 2022). Thus,
 150 the total amount of carbon in the produced slag can be calculated as:

$$151 \quad C_{\text{slag}} = \frac{p_{\text{coke}}}{78.5\%} \times 0.06\% \times 80\% = 0.16 \text{ t C hr}^{-1} \quad (7)$$

152 by substituting Eq. (5), (6) and (7) into Eq. (4), the mass of carbon in the combusted COG
 153 ($C_{combustion-COG}$) during the coking process is calculated to be 27.9 t hr^{-1} . Thus, $E_{combustion-COG}$ and
 154 $E_{combustion-slag}$ can be calculated respectively:

$$155 \quad E_{combustion-COG} = C_{combustion-COG} \times \frac{M_{CO_2}}{M_C} = 102.3 \text{ t CO}_2 \text{ hr}^{-1} \quad (8)$$

$$156 \quad E_{combustion-slag} = C_{slag} \times \frac{M_{CO_2}}{M_C} = 0.59 \text{ t CO}_2 \text{ hr}^{-1} \quad (9)$$

157 where M_{CO_2} and M_C is the molar mass of CO_2 and the atomic mass of carbon, respectively.

158 As certain amount of CO_2 is directly released into the atmosphere along with COG, the carbon mass
 159 in the released and measured CO_2 ($C_{release}$) can be derived as:

$$160 \quad C_{release} = \beta(C_{coal} - C_{coke} - C_{slag}) \times \frac{\varphi_{CO_2}}{\varphi_{CO_2} + \varphi_{CH_4} + \varphi_{CO} + 2\varphi_{C_2H_4}} = 0.16 \text{ t hr}^{-1} \quad (10)$$

161 where β is fraction of COG that is directly released into the atmosphere, taken to be 0.05 as described
 162 above, φ_{CO_2} , φ_{CH_4} , φ_{CO} , and $\varphi_{C_2H_4}$ are the volume fractions for the main constituents in COG (Table
 163 S2). Thus, the corresponding CO_2 emissions from the direct release of COG ($E_{release}$) can be derived as:

$$164 \quad E_{release} = C_{release} \times \frac{M_{CO_2}}{M_C} = 0.59 \text{ t CO}_2 \text{ hr}^{-1} \quad (11)$$

165 by substituting Eq. (8), (9) and (10) into Eq. (3), the total CO_2 emissions (E_{CO_2}) from the full coking
 166 process is calculated to be $103 \text{ t CO}_2 \text{ hr}^{-1}$.

167 Taking into account the variation in carbon content found in both coking coal and coke, the variation
 168 in the fraction of COG used as fuel (assuming a range of 0.4 to 0.6), the uncertainty of slag yield, as well
 169 as the range in the volume fraction of the main components of COG, the total uncertainty range of CO_2
 170 released into the atmosphere during the coking process can be estimated to be 31% by the equation below:

$$171 \quad \delta^2 = \delta_{C_{coal}}^2 + \delta_{C_{coke}}^2 + \delta_{COG \text{ as fuel}}^2 + \delta_{slag \text{ yield}}^2 + \delta_{volume \text{ fraction}}^2 \quad (12)$$

172 Thus, the total amount of CO_2 released into the atmosphere during the full coking process estimated
 173 from the coke production data is $103 \pm 32 \text{ t CO}_2 \text{ hr}^{-1}$, which is consistent with the CO_2 emission results
 174 ($110 \pm 18 \text{ t CO}_2 \text{ hr}^{-1}$, see main text) from the current UAV-measurements.

175 References

176 Dai, X., Li, D., Li, P., Liu, Y., Guo, D., Zhao, P., and Zhang, Y.: Characterization of microscopic structure
 177 and analysis of coking process for various coking coals, *Ironmaking & Steelmaking*, 1-5,
 178 10.1080/03019233.2022.2102886, 2022.

179 Gordon, M., Li, S. M., Staebler, R., Darlington, A., Hayden, K., O'Brien, J., and Wolde, M.: Determining
180 air pollutant emission rates based on mass balance using airborne measurement data over the Alberta oil
181 sands operations, *Atmospheric Measurement Techniques*, 8, 3745-3765, 10.5194/amt-8-3745-2015,
182 2015.

183 Hein, M. K., Manfred: *Environmental Control and Emission Reduction for Coking Plants*,
184 10.5772/48275, 2012.

185 Li, J. L., P.; She, X.; Tu, Z.; Wang, J.; Xue, Q.: Pyrolysis and kinetic analysis of tar residue, *Modern*
186 *Chemical Industry*, 42, 108-118, 10.16606/j.cnki.issn0253-4320.2022.S2.024, 2022.

187 Razzaq, R., Li, C., and Zhang, S.: Coke oven gas: Availability, properties, purification, and utilization in
188 China, *Fuel*, 113, 287-299, 10.1016/j.fuel.2013.05.070, 2013.

189 U.S. Environmental Protection Agency (EPA): 12.2 Coke Production Final May.
190 https://www.epa.gov/sites/default/files/2020-11/documents/c12s02_may08.pdf, 2008

191 Yang, Y.: A UAV based 3-D wind measurement methodology for applications to air pollutant emission
192 quantification, in preparation for submission to *Environmental Science and Technology*, 2023.

193 Zhang, Y.: Review on the Current Status of Coke Oven Gas Utilization in China, *Shandong Chemical*
194 *Industry*, 48, 172-173, 10.19319/j.cnki.issn.1008-021x.2019.16.072, 2019.

195